ARCHITECTURE CIVIL ENGINEERING ENVIRONMENT
The Silesian University of Technology No. 2/2024

doi: 10.2478/ACEE-2024-0016

HYGROTHERMAL DESIGN OF CONNECTIONS IN WALL SYSTEMS INSULATED FROM THE INSIDE IN HISTORIC BUILDING

Bożena ORLIK-KOŻDOŃ*

[a] PhD Eng.; Faculty of Civil Engineering, Silesian University of Technology, Akademicka 5 ,44 – 100 Gliwice, Poland
*E-mail address: *Bozena.Orlik-Kozdon@polsl.pl*

Received: 17.10.2023; Revised: 3.04.2024; Accepted: 3.06.2024

Abstract
The article presents selected issues related to raising energy standards of historical buildings. Due to their unique character, i.e. historic facades and architectural and decorative elements, the use of typical wall insulation methods, e.g. the ETICS system (External Thermal Insulation Composite Systems), is not possible. One solution is to insulate the external envelopes from the inside. Such an internal application method of insulation in the wall system has a significant impact on the profile of the occurring hygrothermal processes and it can trigger many unfavorable phenomena across the surface of the envelope. The design process and the selection of the type and thickness of insulation are carried out in accordance with commonly used criteria and principles – analogous to those used for newly designed buildings such as meeting minimum thermal insulation defined by the coefficient U and eliminating the risk of surface or interstitial condensation.
In thermal insulation systems from the inside, due to the specificity of the solution (lack of the continuity of thermal insulation), special attention should be paid to the places of connections and nodes in the insulated wall systems. Due to the lack of clearly defined criteria for designing such areas and insufficiently identified nature of hygrothermal processes occurring there, the following objectives were set in the work:
- **identification and assessment of thermal insulation solutions within the selected 2D and 3D connections in thermal insulation systems from the inside in terms of avoiding adverse hygrothermal phenomena,**
- **indication of problems and threats that go along with such types of thermal modernization works.**

Keywords: **Historical buildings; Internal insulation; 2D/3D connections; Surface condensation; Risk of mold growth; f_{Rsi} factor.**

1. INTRODUCTION

Energy consumption in the contemporary world contributes to pollution, environmental degradation, and global greenhouse gas emissions. The construction sector is the largest single energy consumer in Europe, and it is responsible for approximately 42% of energy consumption and for 35–40% of CO_2 emissions [1, 2, 3, 4, 5]. Based on EU regulations [6], an obligation is being introduced to develop long-term strategies and support for residential and non-residential buildings, so that by 2050 their high energy efficiency corresponding to the standard of buildings with almost zero energy consumption could be achieved [6]. The new regulations include *primarily energy efficiency* [6, 7], and set the target of reducing energy consumption by at least 32.5% by 2030 [6, 7].

The existing building stock contained in the obligation to raise energy standards also includes historical buildings for which scientific research on new solutions to improve energy performance while maintaining their historical value should be supported [6, 7].

The endeavors to raise energy standards of historic buildings must usually be carried out in accordance with the principles of conservation protection. In many cases, due to historic facades of buildings and the need to maintain their architectural character and decorative elements, the use of typical thermal

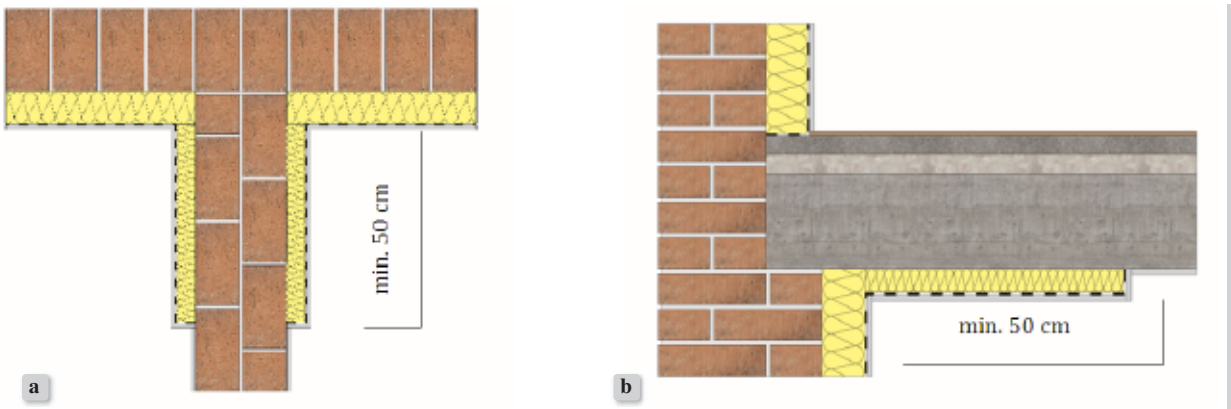

Figure 1.
Graphic solutions of nodes such as: a) connection of the external wall with the internal one, b) connection of the ceiling with the external wall [13, 34, 35]

modernization methods, e.g. wall insulation in the ETICS system (*External Thermal Insulation Composite Systems* [8]), is not possible. The solution is to insulate the external envelopes from the inside. However, this method significantly affects the profile of the occurring hygrothermal processes in the insulated wall systems [9, 10, 11, 12, 13, 14, 15], and it may be conducive to many unfavorable phenomena. The main threats comprise interstitial condensation and increased moisture in the layers of the wall system [16, 17, 18, 19, 20] as well as the risk of frost damage [21, 22, 23, 24, 25], biological corrosion of wooden elements [9, 22, 26, 27, 28] or the development of mold on the internal surface of the envelopes [17, 23, 28, 29]. In such systems, moisture is the main factor that limits the durability of elements and negatively affects the properties of the existing and applied building materials [30, 31, 32].

The reduction of the above-mentioned threats seems to be possible by implementing the requirements for envelopes in terms of hygrothermal design. These include the following criteria [33]:

- meeting the minimum thermal insulation standard of the envelopes with thermal transmittance coefficient U [W/(m^2·K)],
- elimination of the risk of water vapor condensation and the development of mold fungi on the surface of the envelopes,
- elimination of increasing moisture in subsequent years caused by the condensation of water vapor inside the envelope.

The above criteria are usually tested for a flat wall layout, with the exception involving the estimation of surface condensation risk, which is determined for the connections. In thermal insulation systems from the inside, due to the specificity of the solution, local discontinuity of the insulation material may appear in such places (connections, nodes), e.g.:

- due to obstacles such as internal walls or ceiling. It is recommended to make additional insulation along the length of the impact of boundary cooling with a width of at least 50 cm, Fig. 1. The length of the protection can also be determined on the basis of numerical analyses based on the distribution of isotherms in the temperature field. The extent of the area with a non-linear distribution should correspond with the length of the additional protection.
- due to work execution errors – insulation works are often carried out within one apartment and are commissioned following the owners' own initiative. As an example we can mention the so-called boundary (edge) bridges, which are the result of partial insulation of walls and their connections, Fig. 14 [30, 34].

Due to the lack of clearly defined criteria for designing connections in thermal insulation systems from the inside and the so far unidentified nature of hygrothermal processes taking place in such areas, the following objective of the work was set:

- presentation of thermal insulation solutions within the selected 2D and 3D connections in thermal insulation systems from the inside in terms of avoiding adverse hygrothermal phenomena, indicating the problems and threats that accompany such works.

In effect of the work, we suggest a procedure for designing thermal bridges and nodes in wall systems insulated from the inside in historical buildings.

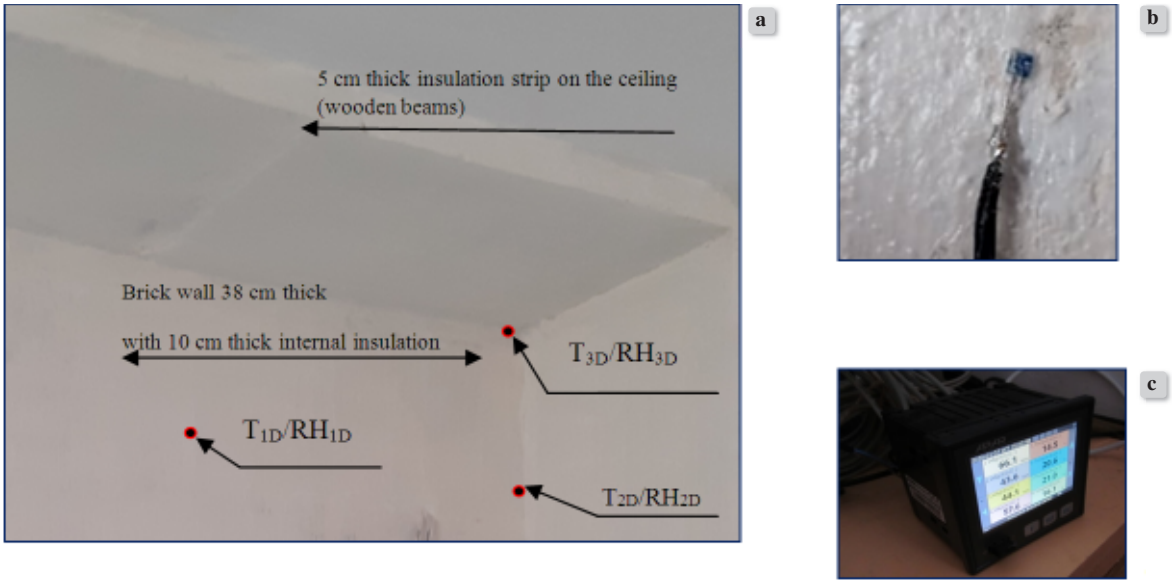

Figure 2.
Test stand: a) location of sensors' installation, b) method of sensors' installation on the surface, (c) data logger

2. MATERIALS AND METHODS

2.1. Test stand

The subject of the research is the analysis and assessment of the distribution of temperature and relative humidity fields on the surface of selected connections in thermal insulation systems from the inside. The connection of two external walls was adopted for the analysis – in the work referred to as a flat corner (marked as 2D) and a spatial corner (marked as 3D).

A flat corner (N2D; xy) is a two-dimensional element that is a connection of external walls away from the influence of elements disturbing the distribution of the temperature field so that the cross-section planes are located at least d_{min} (partition thickness) from the thermal bridge, d_{min} is greater than 1 m and three times greater than the thickness of the element under consideration, the corner model is in accordance with the assumptions of the ISO 10211 standard.

A spatial corner (N3D; xyz) is a three-dimensional element that is a connection of external walls and the inter-storey ceiling (located under the heated storey); the geometric model is limited by the cross-section planes in accordance with the assumptions of the ISO 10211 standard.

The analyzed nodes are located in a real building, which has undergone a comprehensive thermal modernization, including the insulation of external walls from the inside with a 10 cm thick insulator. The building was made in traditional technology with external walls 38 cm and 25 cm thick, made of solid brick with cement-lime mortar, Fig. 2. It has wooden, beam ceilings and new PVC windows. The building has central heating with a solid fuel coal boiler, and convection heaters.

The tests included various types of 2D and 3D connection solutions, i.e. the use of additional wedges along the length of 50 cm, or their complete absence. The case of the so-called edge bridges, i.e. the lack of continuity of thermal insulation over the entire surface of the wall (e.g. due to the existing installation infrastructure and others; a phenomenon common in private buildings).

In light of the above, the following variants of solutions were adopted for testing and analysis, Fig. 3–6:

1. Flat corner – connection of two external walls made of brick, 38 cm thick, with external plaster on both sides without thermal insulation – variant W1,
2. Flat corner – connection of two external walls made of brick, 38 cm thick, with external plaster on both sides with partial insulation – so-called edge bridge – variant W2,
3. Flat corner – connection of two external walls made of brick, 38 cm thick, with double-sided external plaster with thermal insulation, 10 cm thick – variant W3,
4. Spatial corner – connection of the wooden ceiling with the external corner – comprehensive insulation – variant W4.

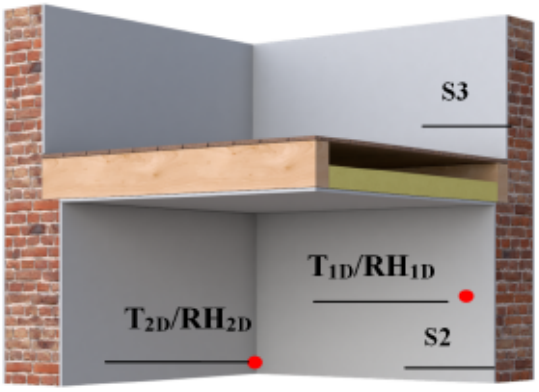

Figure 3.
Flat corner in the non-insulated variant – W1

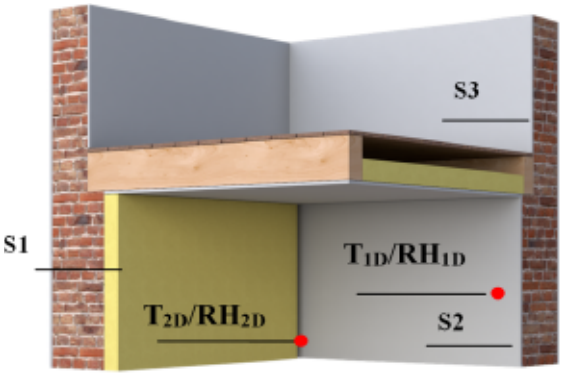

Figure 4.
Flat corner in the partially insulated variant – W2

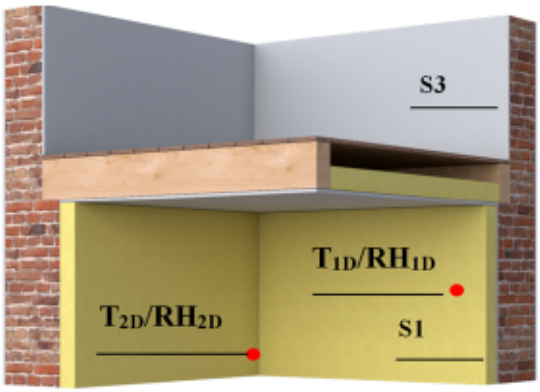

Figure 5.
Flat corner in the insulated variant without ceiling insulation the in the form of strips – variant W3

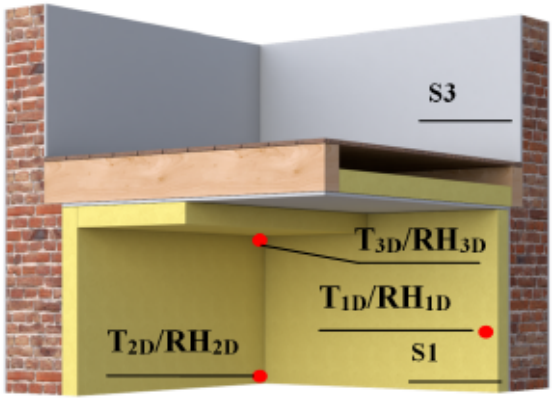

Figure 6.
Spatial corner – variant W4

Fig. 3 shows the illustrations of the analyzed thermal bridges with an indication of the sensor installation locations and the designation of the analyzed parameters (the illustrations indicate the sensor installation locations). For all cases, the numerical analysis described in point 3 was performed.

Material solutions of the wall with its layout of layers are given in Table 1, respectively for the non-insulated wall S_1 and the insulated wall S_2.

Wall S2 – like S1 without thermal insulation with cement-lime plaster.

Wall S3 – a wall made of solid brick, 25 cm thick, with cement-lime plaster on both sides.

2.2. Numerical modelling

The insulation of external envelopes from the inside affects directly the thermal quality of the entire building envelope. These changes are particularly evident at the places of connections and nodes. The use of internal insulation significantly reduces the impact of the intensity of the heat flow coming from the adjacent zones. As a result, the temperature of internal surfaces in the edge zone decreases in relation to the state occurring in analogous thermal conditions

Table 1.
List of thermal and moisture parameters for the wall S1

No.	Layer	Thickness d[m]	Density [kg/m^3]	Thermal conductivity index λ [W/(m·K)]	Diffusion resistance factor μ [–]
1.	Solid brick on cement-lime mortar	0.38	1800	0.60	15.0
2.	Leveling layer of cement-lime plaster	0.015	1900	0.80	19.0
3.	System adhesive mortar	0.01	833	0.015	15.1
4.	Lightweight cellular concrete slabs	0.10	115	0.04	4.1
5.	System finishing layer	0.01	833	0.015	15.1

before thermal insulation. The purpose of the conducted numerical analyses was to determine changes in the temperature field on the surface of the selected thermal bridges. The analyses were conducted on the example of a node of the following type:

- external corner – in various insulation variants – W1, W2, W3,
- ceiling support on the external wall – 3D corner in various insulation variants – W4.

The node models were made in accordance with the assumptions of the ISO 10211 standard.

To develop a suitable solution of a thermal bridge detail which would satisfy the binding hygrothermal regulations, detailed calculations of the following physical parameters were carried out:

- linear thermal coupling coefficient L^{2D} [W/(mK)],
- linear thermal transmittance, defining additional heat losses effected by the presence of linear thermal bridges [W/(mK)] [36]:

$$\psi = L^{2D} - \sum_{j=1}^{N_j} U_j \, l_j \tag{1}$$

where:

L^{2D} – thermal coupling coefficient obtained from the calculations involving the two-dimensional heat flow of the component separating the two investigated environments [W/(mK)],

U_j – thermal transmittance of the one-dimensional j-th component separating the two investigated environments [W/(m^{2}K)],

l_j – length applicable for Uj [m],

N – number of the one-dimensional components.

- temperature factor, defined on the basis of the minimum temperature on the envelope surface at the place of thermal bridge f_{Rsi} [37]:

$$f_{Rsi} = \frac{\theta_{si} - T_e}{T_i - T_e} \tag{2}$$

where:

θ_{si} – calculated temperature of the internal surface at the critical place,

T_i – temperature of indoor air,

T_e – temperature of outdoor air.

3. RESULTS

3.1. In situ measurement

3.1.1. Contact measurements

The study of the connections in the form of flat and spatial corners in thermal insulation systems from the inside was carried out in real operating conditions and included continuous recording of temperature and relative humidity on the surface of the analyzed nodes. The measurements were carried out from 2019 with a time step of 1 hour. The paper presents the results for the selected research period (January). Figs. 7–10 show the profiles of the changes in temperature and relative humidity for variants W1-W4 for the selected research period (January) – all profiles were obtained based on contact measurement with the use of sensors Pt100 and HIH 4000.

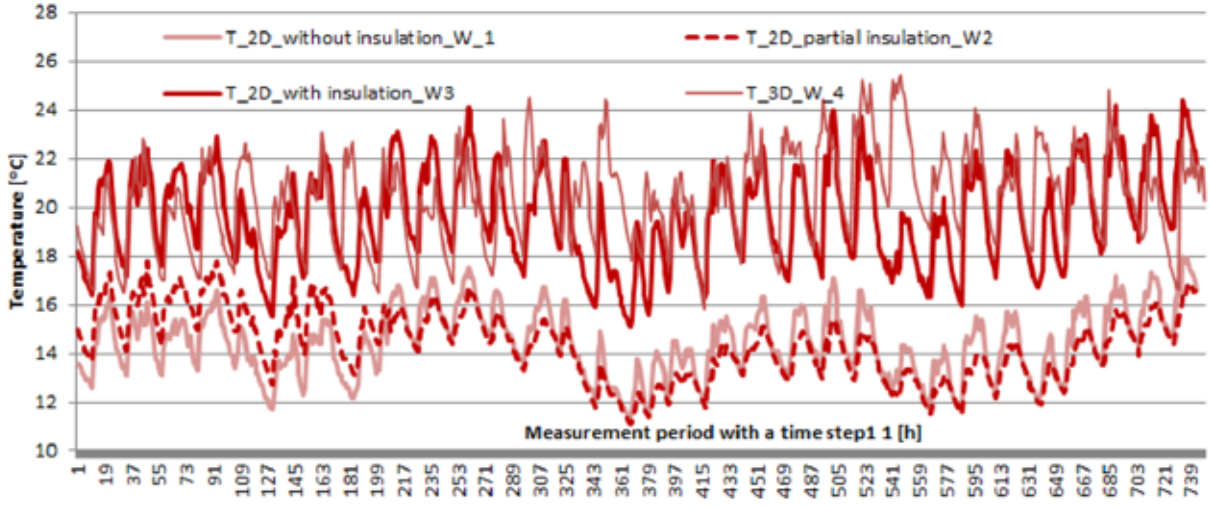

Figure 7.
Profiles of temperature changes on the surface of a flat and spatial corner in variant W1-W4

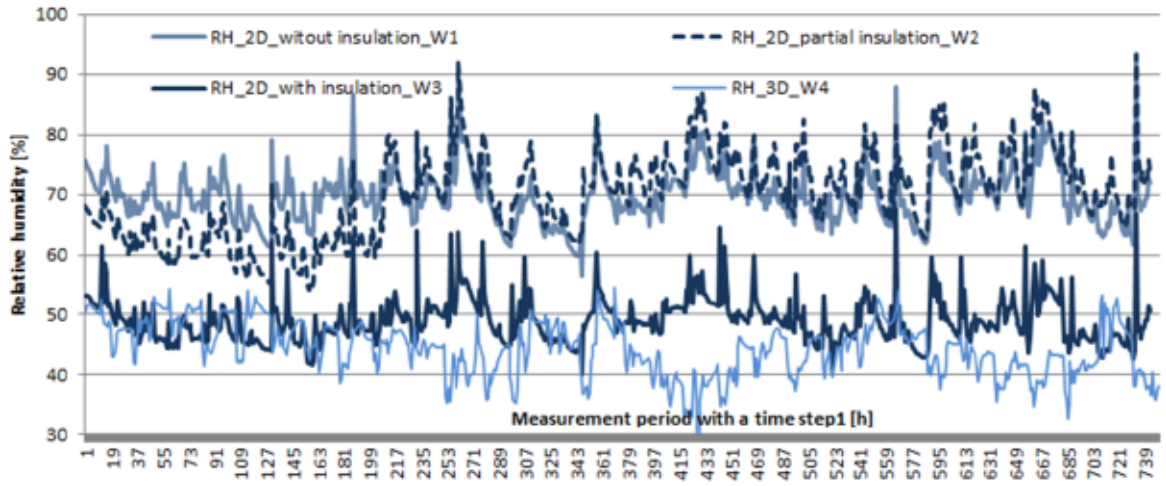

Figure 8.
Profiles of the changes in relative humidity on the surface of a flat and spatial corner

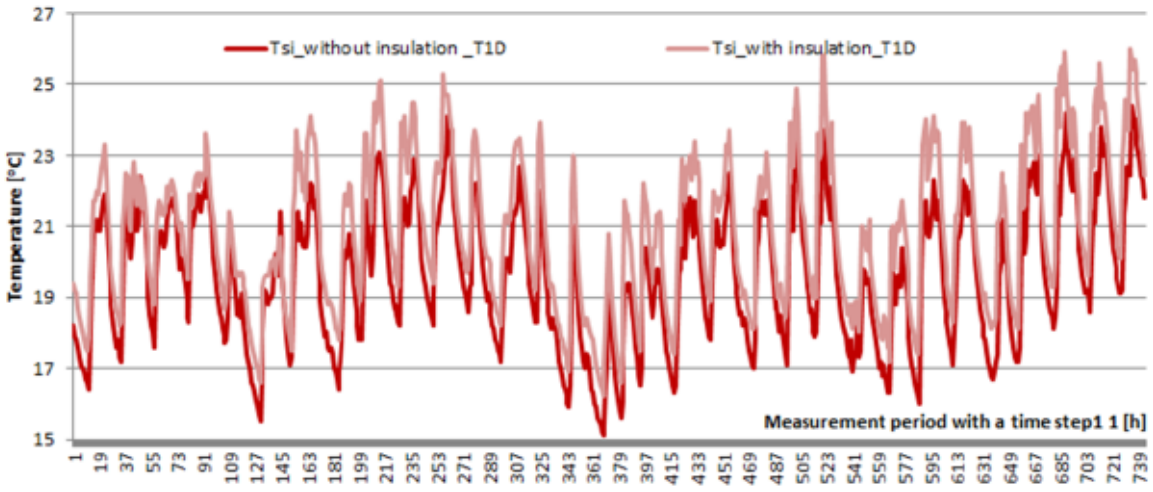

Figure 9.
Profiles of temperature changes on a flat surface

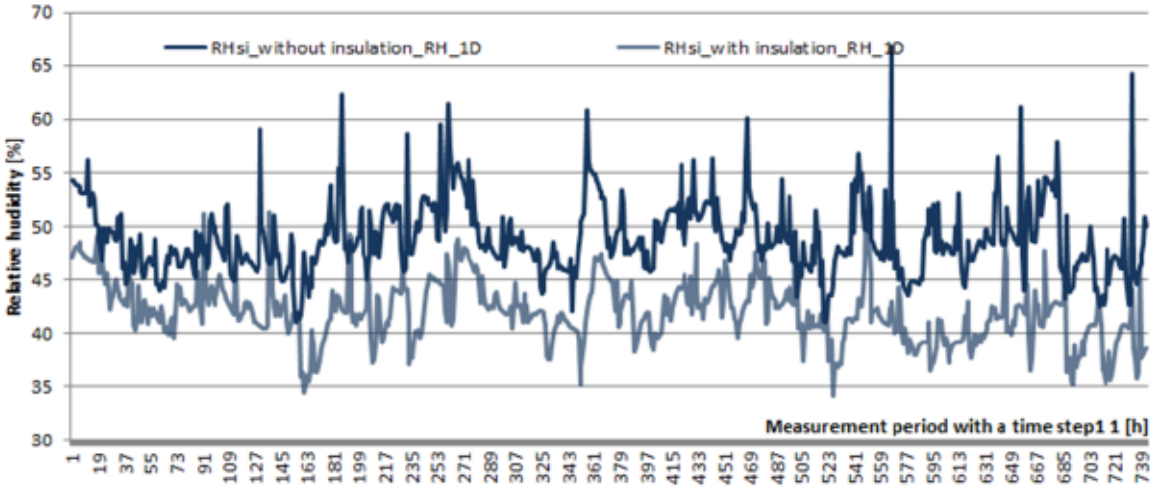

Figure 10.
Profiles of the changes in relative humidity on a flat surface

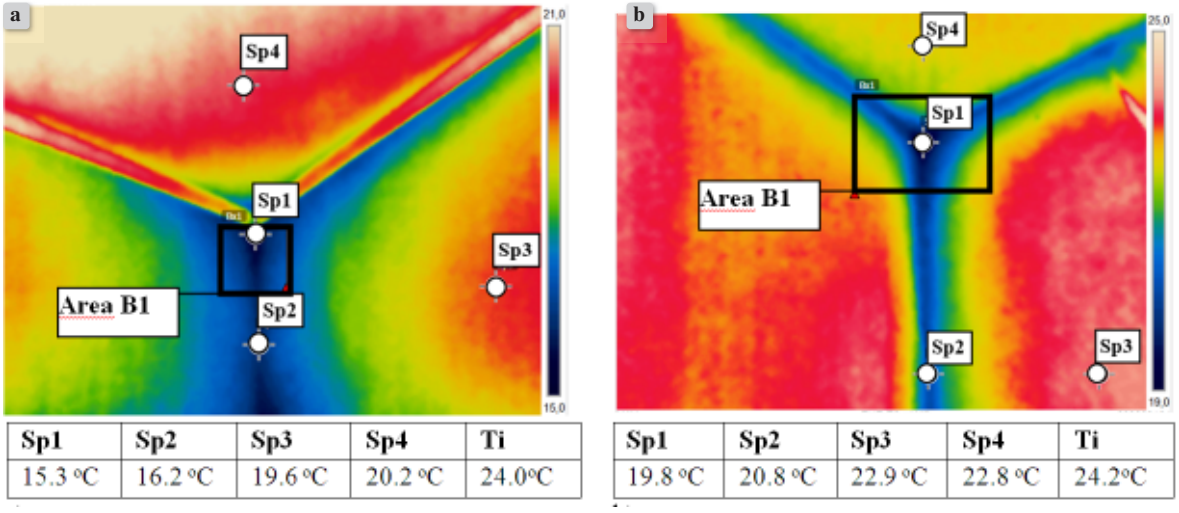

Sp1	Sp2	Sp3	Sp4	Ti
15.3 °C	16.2 °C	19.6 °C	20.2 °C	24.0°C

Sp1	Sp2	Sp3	Sp4	Ti
19.8 °C	20.8 °C	22.9 °C	22.8 °C	24.2°C

Figure 11.
Distribution of surface temperature field for the 3D/2D corner in a historical building: a) non-insulated (with a polystyrene strip minimizing the temperature drop on the edge), b) insulated (with an insulating strip on the ceiling)

Based on the profiles of changes in temperature and relative humidity on the surface of the analyzed nodes, the following was found:

- the maximum surface temperature in the considered period was respectively (for the maximum air temperature in the room T_i = 28°C):
  - for the non-insulated 2D corner: T_{2Dmax} = 18°C ,
  - for the partially insulated 2D corner: T_{2Dmax}=17.8°C,
  - for the insulated 2D corner: T_{2Dmax} = 25.2°C,
  - for the insulated 3D corner: T_{3Dmax} = 25.6°C.
- the maximum relative humidity of the surface in the considered period was respectively (for the maximum relative humidity of the air in the room RH_i = 51.4%):
  - for the uninsulated 2D corner: RH_{2Dmax} = 93.5%,
  - for the partially insulated 2D corner: RH_{2Dmax} = 93.2%,
  - for the insulated 2D corner: RH_{2Dmax} = 67.7%,
  - for the insulated 3D corner: RH_{3Dmax} = 54.5%.

The average surface temperature difference between the insulated and non-insulated corner was 5.7°C, and in the case of relative humidity it was 20.8%.

It should be noted that the relative air humidity levels for the non-insulated and partially insulated corners exceed the permissible humidity threshold of 80%, after which the risk of mold growth increases [30, 34, 35].

3.1.2. Remote measurements

The determination of the temperature field distribution on the surface of the wall systems was made by means of remote measurement using a FLIR E8 thermal imaging camera with the following specifications: thermal sensitivity of the camera of 0.06°C, resolution of 320 x 240; measuring range from -20°C to 250°C; camera angle of view of 45° x 34°. Thermal imaging tests were carried out at the external air temperature T_e = (-1.2)°C and the measured emissivity ε = 0.95.

The aim of the research was to visualize the temperature field:

- on the surface of spatial corners (T_3D) and flat corners (T_2D) in variants W1 and W3. On the thermogram (Fig. 11) we can see a color visualization of the temperature field and its graphic form (Figs. 12, 13),
- on the surface of the flat corner in variants W2 (comprehensive insulation of the corner) and W3 (edge bridge).

In all types of buildings there is a temperature difference between the points Sp1÷Sp2. Quantitatively, its value depends on the thermal quality of the analyzed systems and indoor climatic conditions, Tab. 2.

The thermal imaging tests for flat corners and edge bridges are presented in the thermograms in Fig. 14. All of them show the measurement area 1.2 m above the floor.

Based on the obtained results, the following was found:

- lack of continuity of the insulating material caused local drops in surface temperature,

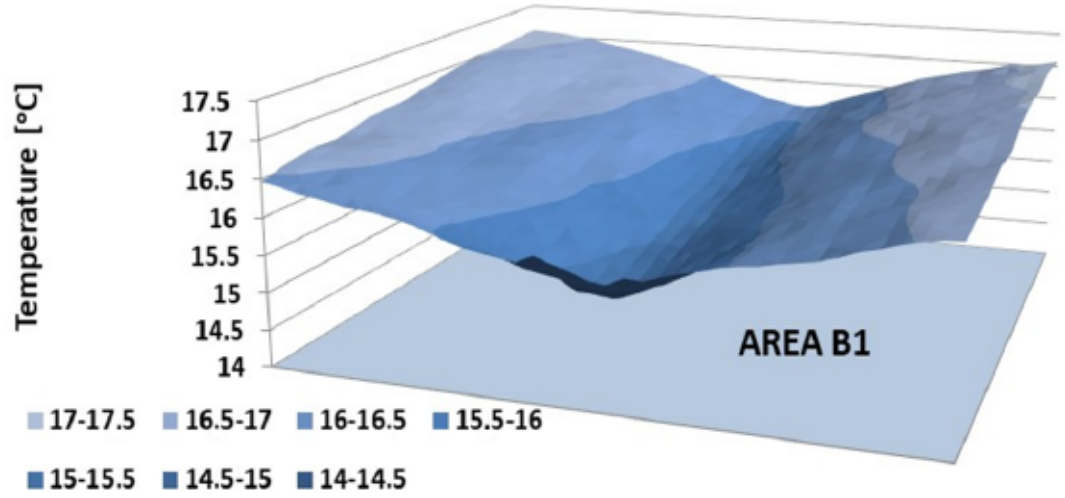

Figure 12.
Distribution of temperature field in the B1 area for the non-insulated 3D/2D corner in a historic building without insulation

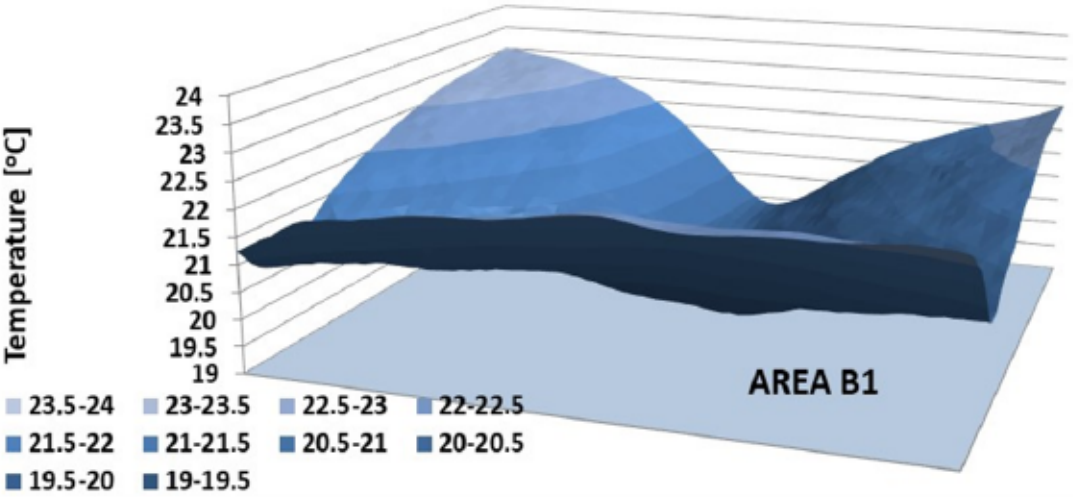

Figure 13.
Distribution of temperature field in the B1 area for the 2D/3D insulated corner in a historic building insulated from the inside

Table 2.
Differences in surface temperature values of the tested corner systems

	Surface temperature difference ΔT [°C]		
	Sp3–Sp1	Sp3–Sp2	Sp2–Sp1
Historic building	4.3	3.4	0.9
Historic building with thermal insulation of the envelopes	4.7	3.1	1.6

- for the partially insulated external corner, we observed a local impact of the defect on the non-insulated external wall, manifesting itself in the form of a wide and irregular area with reduced temperature – the surface temperature at this place was by 7.7°C lower than that on the surface of the insulated wall and by 1.2°C lower than that on the non-insulated wall outside the disturbance area; the temperature in the corner itself had the value T_{si} = 13.5°C at the time of measurement.

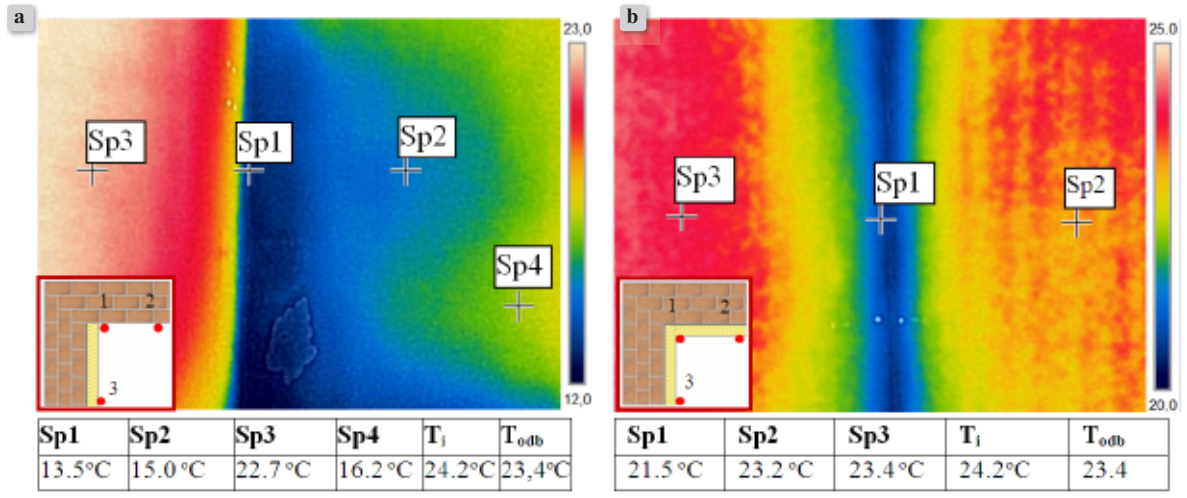

Sp1	Sp2	Sp3	Sp4	T_i	T_{odb}
13.5°C	15.0 °C	22.7 °C	16.2 °C	24.2°C	23,4°C

Sp1	Sp2	Sp3	T_i	T_{odb}
21.5 °C	23.2 °C	23.4 °C	24.2°C	23.4

Figure 14.
Distribution of temperature field on the surface of: a) 2D partially insulated corner, b) 2D fully insulated corner [30]

3.2. Numerical modelling

The numerical analyses of changes in the temperature field on the surface of the selected connections of the wall system insulated from the inside were performed using the programs THERM 7.6 and Psi-Therm 3D.

The adopted input data:

- thermal parameters of the system components are given in Tables 1, 4.
- insulation thickness from 2 cm to 12 cm with gradation every 2 cm (lambda of the insulation $\lambda = 0.04$ [W/(m·K)]), thermal resistance R from 0.0 [(m^2·K)/W] to $R = 3.0$ [(m^2·K)/W],
- strips of the insulating material on the internal wall were equal to the basic thickness of the insulation on the external wall; the strip length in each case was 50 cm,
- external wall made of brick 38 cm thick, internal wall made of brick 25 cm thick.

The adopted assumptions:

- internal temperature was assumed as constant $T_i = 20$°C,
- external temperature was assumed as constant $T_e = (-20$°C),
- heat transfer coefficients on the surfaces: $h_i = 7.69$ [W/(m^2·K)], $h_e = 25$ [W/(m^2·K)], for surface codensation $h_i = 4.0$ [W/(m^2·K)].

Figs. 15, 16 show the selected graphical results presenting the distribution of isotherms in the node as well as heat flux densities for the solutions with edge bridges. In all illustrated cases, the insulation thickness was 10 cm. The calculation results for all analyzed systems are presented in Figs. 5–19. The temperature was read at the points indicated in Figs. 15, 16.

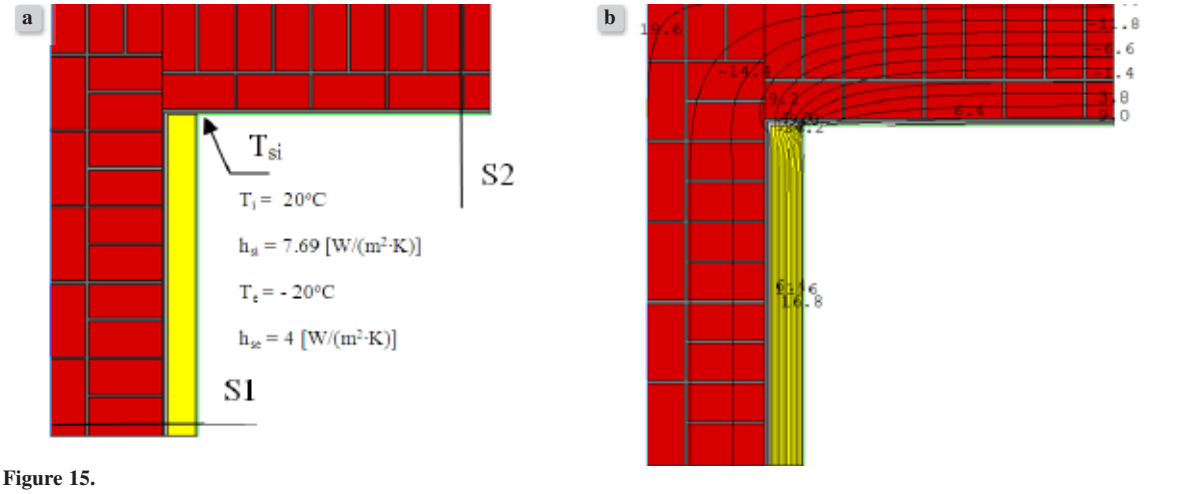

Figure 15.

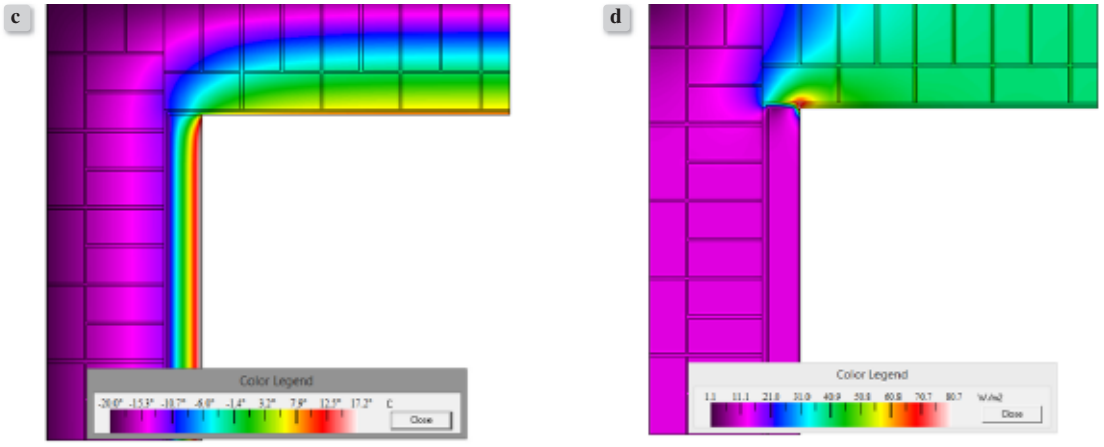

Figure 15.
Results of numerical calculations for the external corner, with partial insulation 10 cm thick: a) node model, b, c) distribution of isotherms, d) distribution of heat flux density

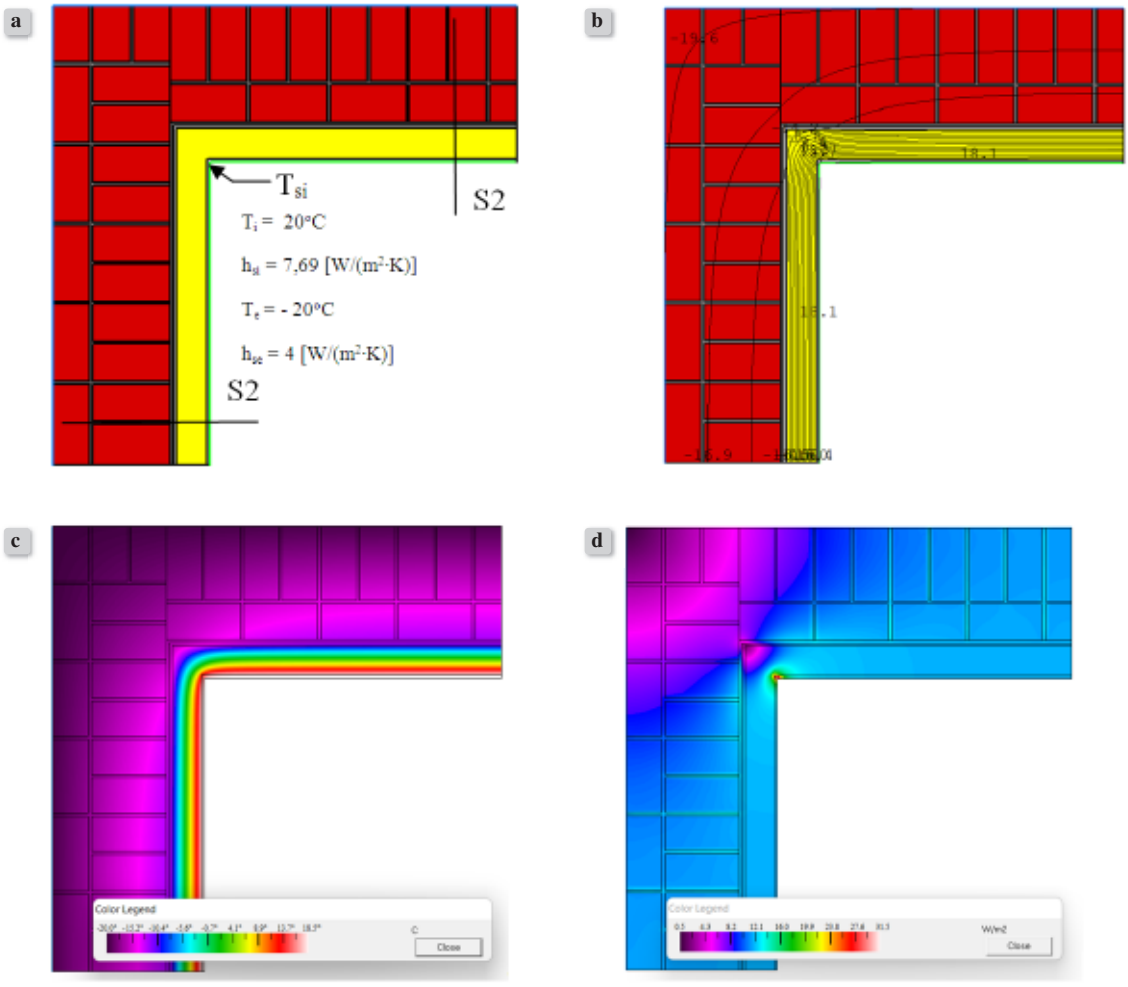

Figure 16.
Results of numerical calculations for the external corner, with comprehensive insulation 10 cm thick: a) node model, b, c) distribution of isotherms, d) distribution of heat flux density

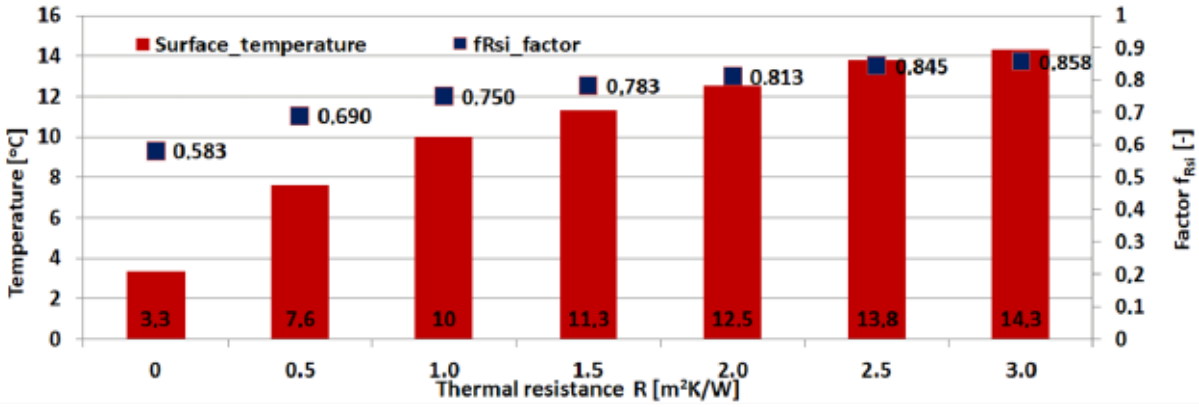

Figure 17.
Surface temperature changes and the effective value of the f_{Rsi} factor for insulated outer corner

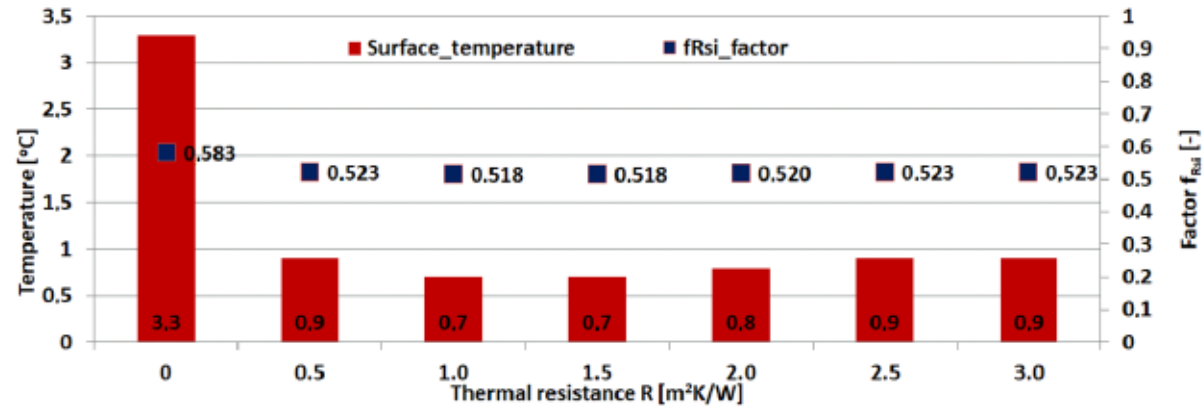

Figure 18.
Surface temperature changes and the effective value of the f_{Rsi} factor for a partially insulated outer corner

The following can be observed based on the presented results:

- the edge bridge in the outer corner causes a rapid temperature drop at the edge (maximum temperature for thermal resistance of the insulation R = 3.0 [(m^2·K)/W] is approx. 1°C) in relation to the solution without insulation (3.3°C); for each insulation thickness there is a risk of mold development at the edges,
- for the insulated corner and for the insulation thickness > 6 cm, the effective value of the f_{Rsi} factor is greater than the limit value referred to in the Technical Conditions [33] (the f_{Rsi} value > 0.72),
- edge zones should always be extended by the so-called strips or wedges made of insulating material along the width of the boundary cooling effect – the extent of the cooling zone is calculated on the basis of numerical calculations; in any other case, min. 50 cm should be assumed.

In addition to the presented changes in the temperature field on the surface of the analyzed details, the linear thermal transmittance coefficient ψ was calculated, which characterizes the so-called linear thermal bridges. The calculations were carried out for external dimensions "*e*". The linear thermal transmittance coefficient was calculated for the entire node (without division into arms).

The calculation results are presented in Table 3.

Table 3.
Cumulative results of corner calculations

Thermal resistance of insulation R [(m^2·K)/W]	Thermal coupling coefficient L_{e2D} [W/(m·K)]		Linear thermal transmittance coefficient ψ_e[W/(m·K)]	
	Insulated corner	Partially insulated corner	Insulated corner	Partially insulated corner
0	2.952	2.952	-0.578	-0.578
0.5	1.672	2.230	-0.460	-0.634
1.0	1.201	2.015	-0.385	-0.599
1.5	0.932	1.882	-0.330	-0.471
2.0	0.758	1.787	-0.290	-0.459
2.5	0.626	1.707	-0.270	-0.464
3.0	0.552	1.655	-0.230	-0.458

e – external dimensioning

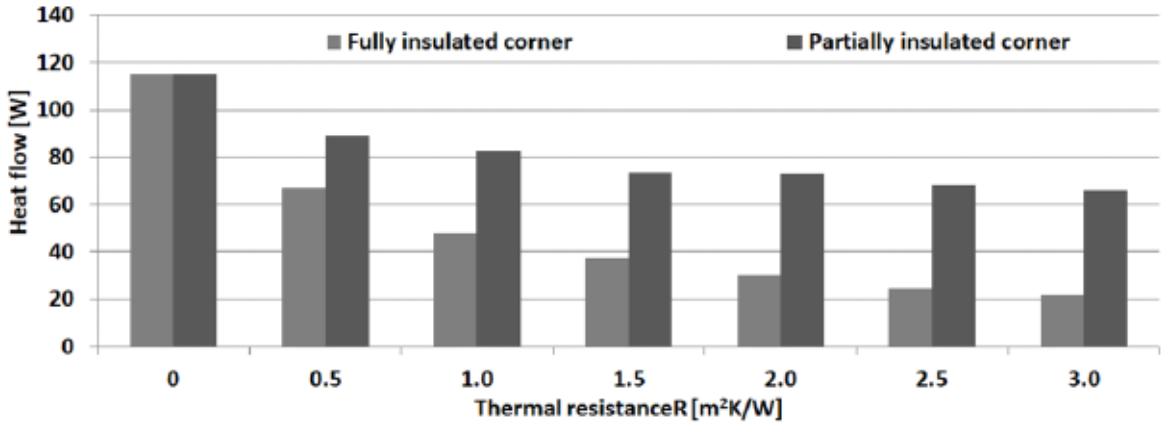

Figure 19.
Results of numerical calculations for the external corner, with partial insulation 10 cm thick: a) node model, b, c) distribution of isotherms, d) distribution of heat flux density

Based on the obtained results, the following can be observed:

- the method of locating the insulation at the place of the so-called thermal anomalies,

The so called geometric bridges causes local disturbances in the heat flux flow,

- comprehensive insulation of external corners significantly reduces heat loss in the node,
- for external corners, regardless of the method of insulation layout or its absence, the value of the linear thermal bridge takes a negative value - for external dimensioning,
- the linear value of the bridge depends on the dimensioning method; the total external dimensioning system is most often used in order to ignore the influence of a significant part of the bridges on the design heat demand.

In order to track the changes in the temperature field at the place of the so-called spatial corners, i.e. the connection of the ceiling with the external wall, calculations were made in the *Psi Therm* program. The modeling of the detail geometry in the form of 3D nodes was performed in accordance with the assumptions of the standard ISO 10211. The calculations were made for the connection illustrations shown in Figs. 20–26, i.e. for a brick wall with a thickness of 38 cm (ground floor) / 25 cm (first floor) combined with an interfloor ceiling (wooden, beam one with a 10 cm thick insulation between the beams) separating the heated rooms. The analyses were carried out in various insulation variants, i.e.:

- wall-ceiling connection in a non-insulated building, variant no. W1,
- wall-ceiling connection in a building partially insulated from the inside, variant no.W2,
- wall-ceiling connection in a building insulated from the inside on the ground floor, without insulating strips on the ceiling, variant no. W3,
- wall-ceiling connection in a building insulated from the inside on the ground floor, with insulation strips on the ceiling, variant no. W4,
- wall-ceiling connection in a building fully insulated from the inside, variant no. W4_1,
- wall-ceiling connection in a building insulated from the outside, variant no. W5.

The material data of the layers in the node is given in Table 4.

Table 4.
Thermal conductivity of the materials used to build the model

	Brick wall	Plaster	Thermal insulation	Wooden beam	Plaster boardd	OSB plate
λ	0.77	1.00	0.04	0.16/0.13	0.32	0.13
d [m]	0.38/0.25	0.15	0.10	0.14x0.20	0.0125	0.02

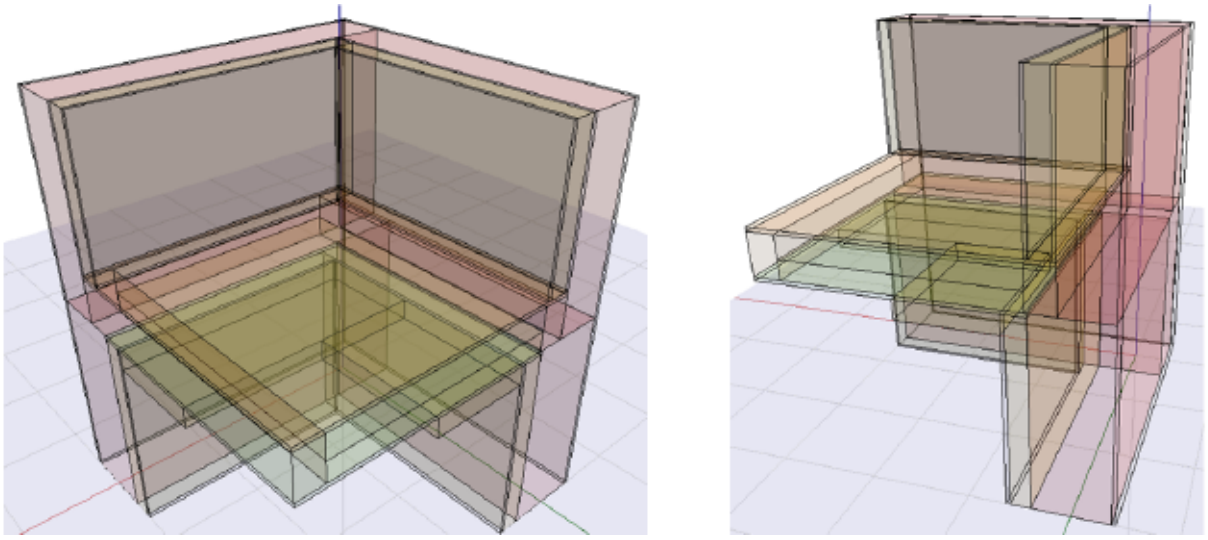

Figure 20.
Schematic of the model for variant W4

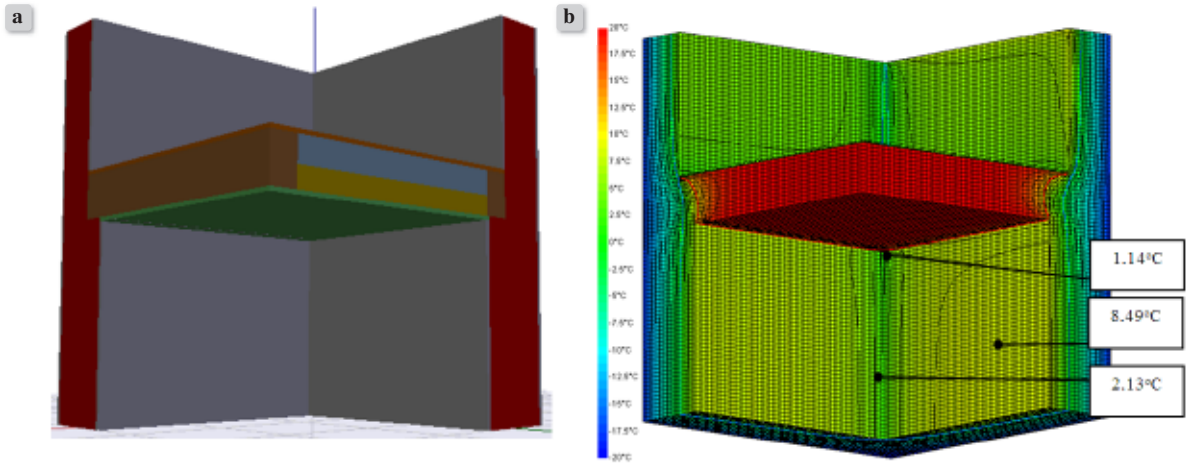

Figure 21.
Envelope model – non-insulated brick wall – W1. Distribution of isotherms in the node

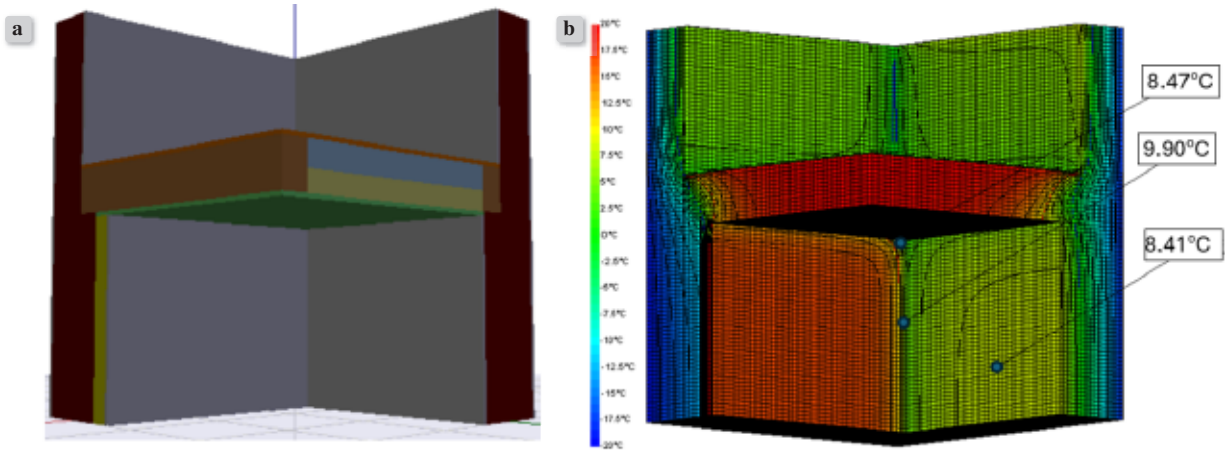

Figure 22.

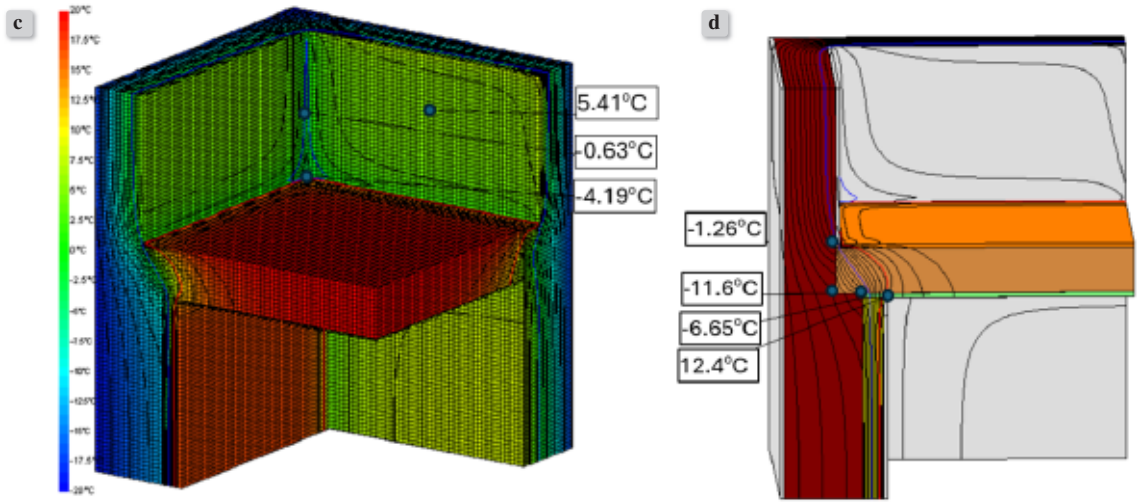

Figure 22.
Envelope model – insulated brick wall – W2. Distribution of isotherms in the node: a), b) top, c) bottom, d) cross-section

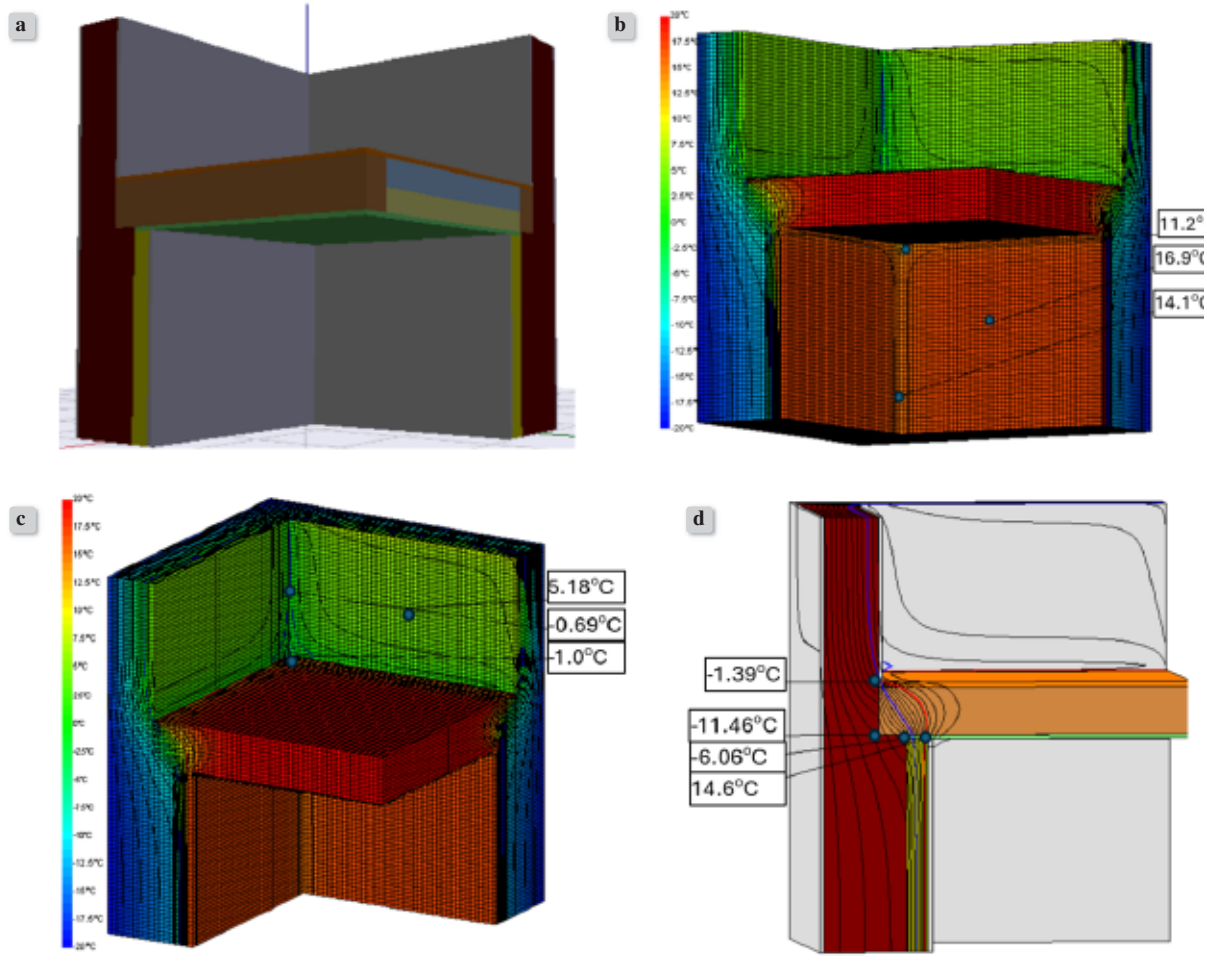

Figure 23.
Envelope model – insulated brick wall – W3. Distribution of isotherms in the node: a), b) top, c) bottom, d) cross-section

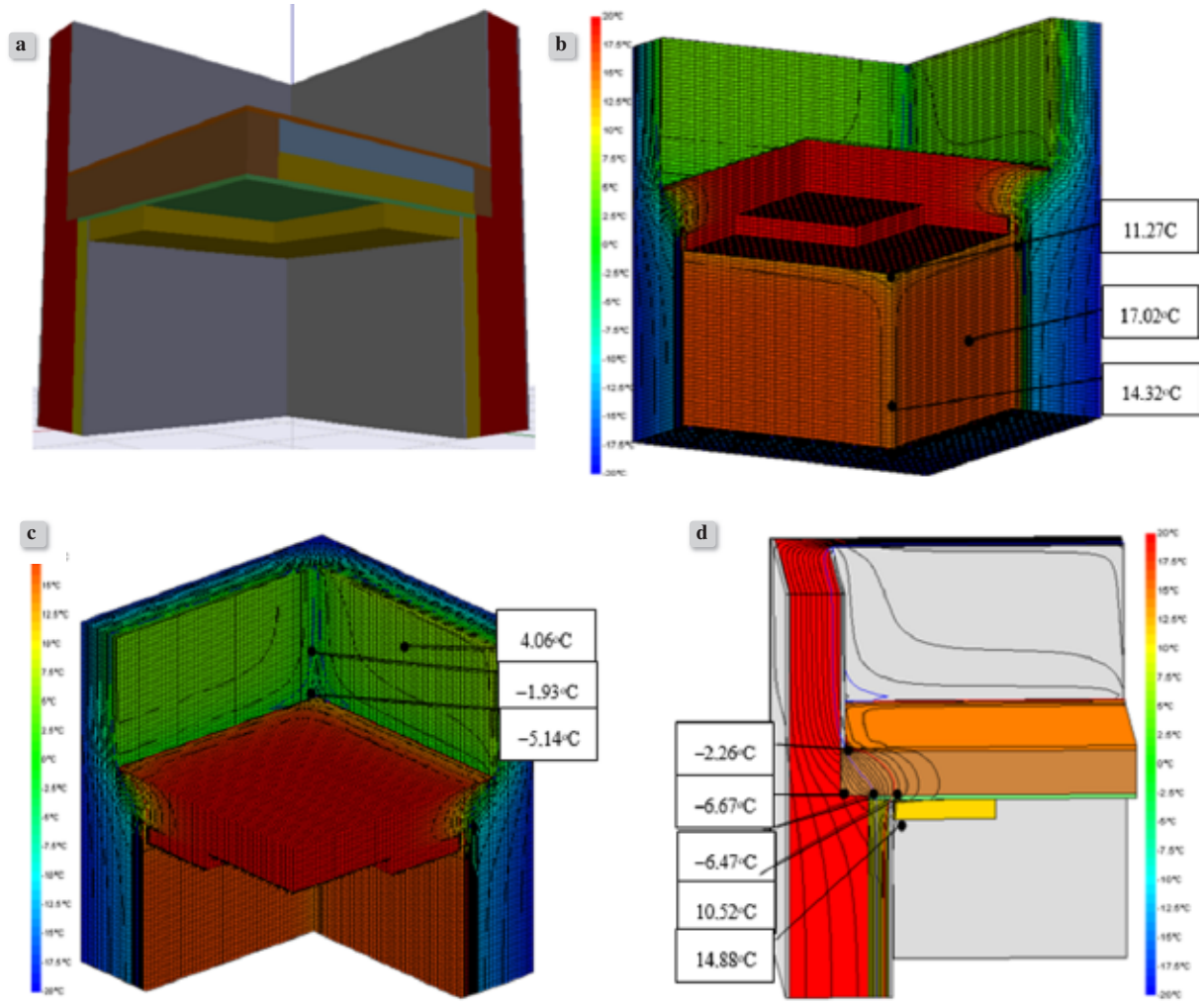

Figure 24.
Envelope model – insulated brick wall – W4. Distribution of isotherms in the node: a), b) top, c) bottom, d) cross-section

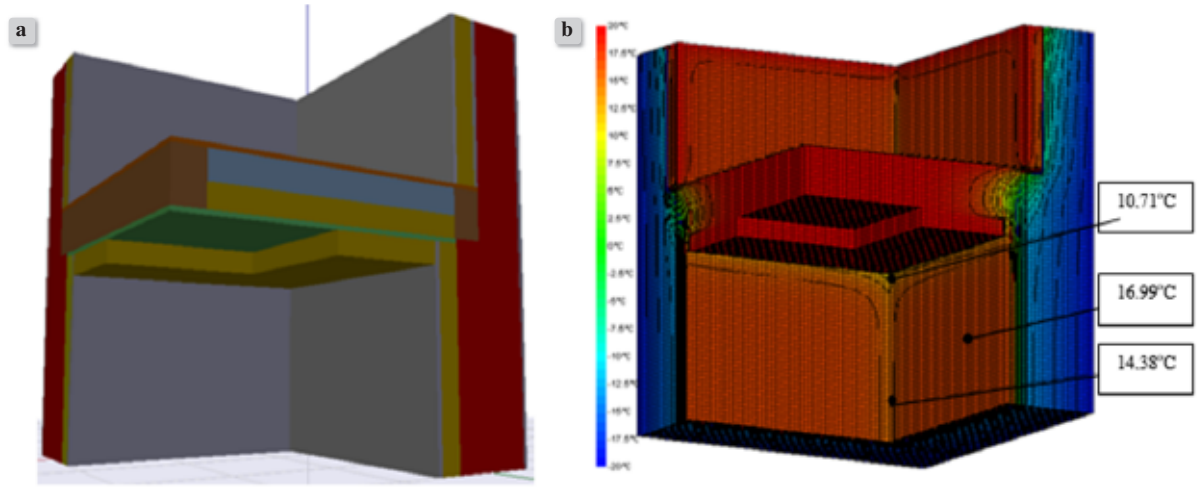

Figure 25.

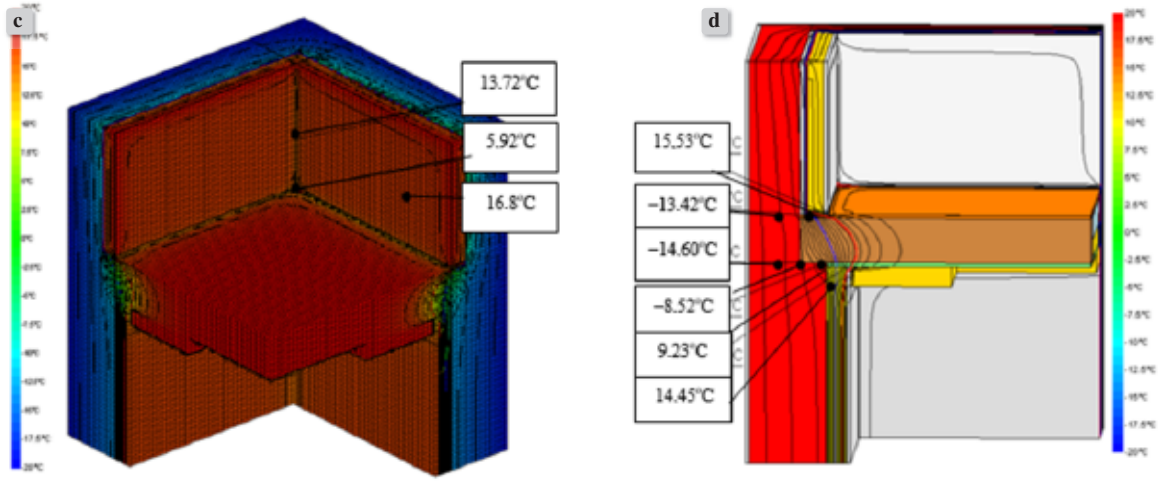

Figure 25.
Envelope model – insulated brick wall – W4_1. Distribution of isotherms in the node: a), b) top, c) bottom, d) cross-section

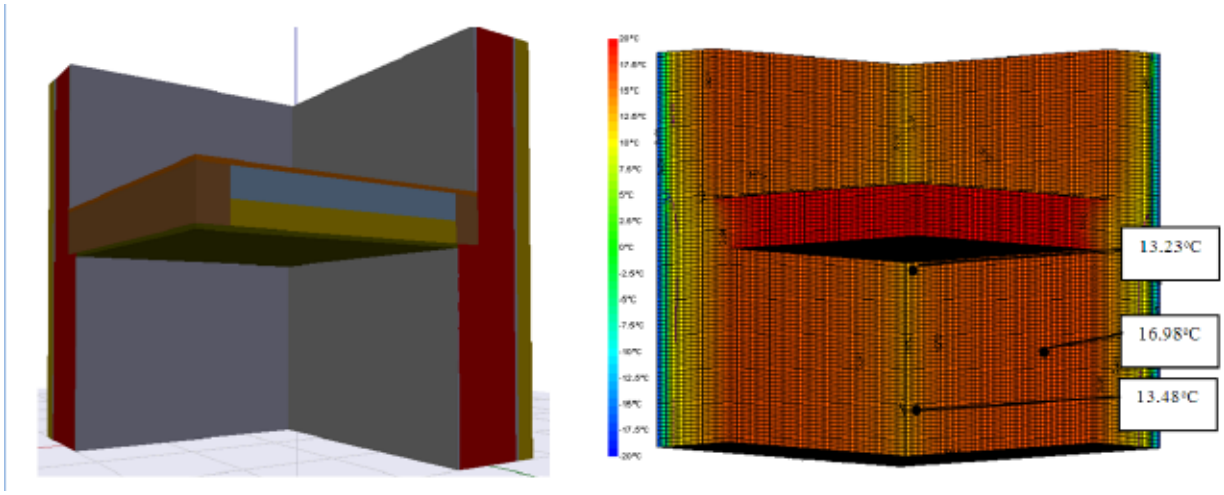

Figure 26.
Envelope model – insulated brick wall – W5. Distribution of isotherms in the node

Table 5.
Summary of surface temperature values and f_{Rsi} factor at places T1D/T2D/T3D for variants of the *W1÷W5* system

	Temperature [°C]					Factor f_{Rsi} [–]				
	W1	W2	W3	W4	W5	W1	W2	W3	W4	W5
T1_g	8.49	8.41	16.90	17.02	16.98	0.712	0.710	0.923	0.925	0.925
T2_g	2.13	9.90	14.10	14.32	13.48	0.553	0.748	0.853	0.858	0.837
T3_g	1.14	8.47	11.20	11.27	13.23	0.529	0.648	0.780	0.782	0.831
T3_d	–4.21	–4.19	0.00	–5.14	11.69	0.395	0.442	0.475	0.372	0.792

*T1_g - temperature of flat_top surface, T2_g - temperature of 2D_top corner,
T3_g - temperature of 3D_top corner, T3_d - temperature of 3D_bottom corner.

For all four connection variants (*W1÷W5*) based on the obtained results of the modeling of the temperature fields on the surface of the nodes, the temperature factor was calculated at the places T1_g, T2_g, T3_g, T3_d (g- top, d- bottom) for the insulation thickness of 10 cm (R= 2.5 [(m^2·K)/W]. The results are presented in Table 5.

The most advantageous variant in terms of the location of insulation is to insulate the walls from the outside. The envelope and its nodes are protected

against the risk of mold growth (for the insulation thickness of 10 cm). This conclusion is correct assuming that $f_{Rsi,max}$ is equal to 0.72 (the value given in the Technical Conditions [33] for the temperature of 20°C and air humidity RH_i of 50%).

In the case of variants W4 and W3, there is a risk of surface condensation and mold growth in the 3D corners (bottom) due to local temperature drop at the edge.

For variant no. W1 and its nodes, the temperature on the surface is lower than the dew point temperature t_s = 10.7°C for the assumed climatic conditions. In that case (no wall insulation) the f_{Rsi} factor does not meet the requirements, there is a risk of mold development on the surface of the envelope and in its nodes.

Table 6 lists the surface temperature values (for all measurement points) for the variant with internal insulation, i.e. variant W4.1 with comprehensive insulation and variant W4 with the insulation of the floor.

When analyzing the obtained results of surface temperatures for the variants with insulation from the inside, we observe that the front of the wooden beam for the given boundary conditions is always within the range of negative temperatures. Comprehensive insulation of the node and the building allows to obtain the surface temperature in the 2D corners (ground floor, first floor) above the minimum surface temperature, and thus eliminates the risk of mold growth. The insulation applied within one apartment significantly changes the surface temperature at the place of 3D spatial corners. The application of internal insulation significantly reduces the intensity of heat flow coming from the adjacent zones, which is observable in the temperature values in the upper 3D corner for variants W4.1 and W4.

For the 3D corners in the systems insulated from the inside, there is a local, edge decrease in surface temperature, Fig. 27. Changes in the temperature field on the inner surface of the node are directly related to the changes in the indoor temperature T_i and outdoor temperature T_e. In the case of the latter (T_e), the impact is much greater due to low thermal resistance of the structural part of the wall system. The contact temperature between the wall and the insulation layer is only slightly higher than the outdoor temperature.

Table 6.
Temperature values at the points W4 and W4.1 indicated on the details

Location		Temperature at point [°C]	
		Variant W4_1	Variant W4
Beam support	T1	–13.42	–2.26
	T2	–14.6	–6.67
	T3	–8.52	–6.47
	T4	9.23	10.52
	T5	15.53	–
	T6	14.45	14.88
Node 3D_ (bottom)	T1	16.80	4.06
	T2	13.72	–1.93
	T3	5.92	–5.14
Node 3D_ (top)	T1	16.99	17.02
	T2	14.38	14.32
	T3	10.71	11.27

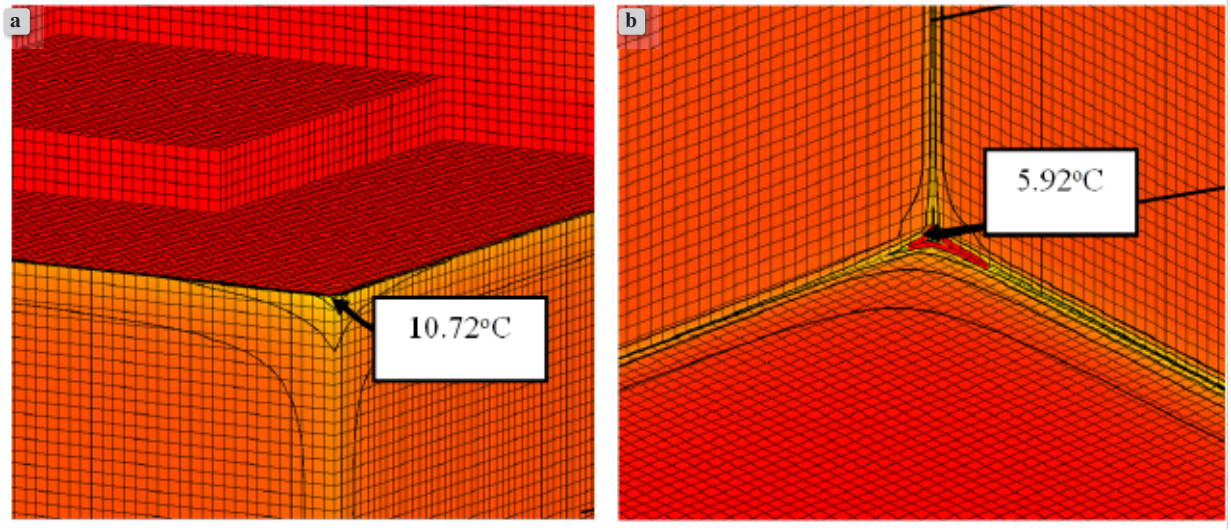

Figure 27.
Local changes in the temperature field for the detail W4_1, in the 3D node: a) top, b) bottom

Conclusions from the conducted numerical analyses:

- on the basis of the obtained temperature values, significant differences in temperature are found on the surface of the 3D corners – due to the location (upper and lower corners) and the extent of insulation (overall insulation of the building or within one floor),
- the application of insulation from the inside causes a local temperature drop below 0°C (for the given boundary conditions); this results not only in the condensation of water vapor, but also in the freezing of the resulting water,
- the assessment of the risk of surface condensation in thermal insulation systems from the inside should be carried out in relation to the entire building envelope, especially when thermal modernization works are carried out within one apartment.

4. SUMMARY

The paper presents selected studies and analyses related to the design and assessment of solutions in the area of connections in wall systems insulated from the inside. They included, among others, measurements of the distribution of temperature and relative humidity on the surface of selected nodes in real operating conditions in a building subjected to thermal modernization. Based on them, the following was found:

- spot measurements of temperature and relative humidity showed a rapid decrease in temperature in the area of the so-called edge bridges and a rise of relative humidity on the surface to a level conducive to the development of mold, i.e. RH>80%,
- comprehensive insulation of the connections and the use of wedges eliminates the development of surface condensation and guarantees the acquisition of surface temperature at the level of the minimum temperature eliminating the risk of mold growth.

The in situ research was supplemented by numerical analyses of the temperature field distribution on the surface and in the area of 2D and 3D connections using Therm and PsiTherm software. Based on them, the following was found:

- the quality of the connection is determined principally by the elimination of the risk of mold growth expressed by the effective f_{Rsi} factor. This assessment should be carried out for the connections in question against the background of the entire building, or at least the adjacent rooms. Internal insulation reduces the impact of the intensity of the heat flow coming from the adjacent zones, which should be taken into account when conducting this type of thermal retrofit works.
- the use of wedges and strips as well as a comprehensive insulation of thermal bridges significantly reduces heat loss. The influence of the thermal bridge expressed by the linear thermal transmittance coefficient is a quantity that is difficult to interpret due to different methods of connection dimensioning and the lack of obligatory limit values for this quantity. The effect is possible to define only at the stage of preparing the building's energy balance when calculating the heat loss coefficient through transmittance.
- the work introduces the concept of effective insulation thickness, i.e. the thickness for which the criteria guaranteeing thermal quality of the connection

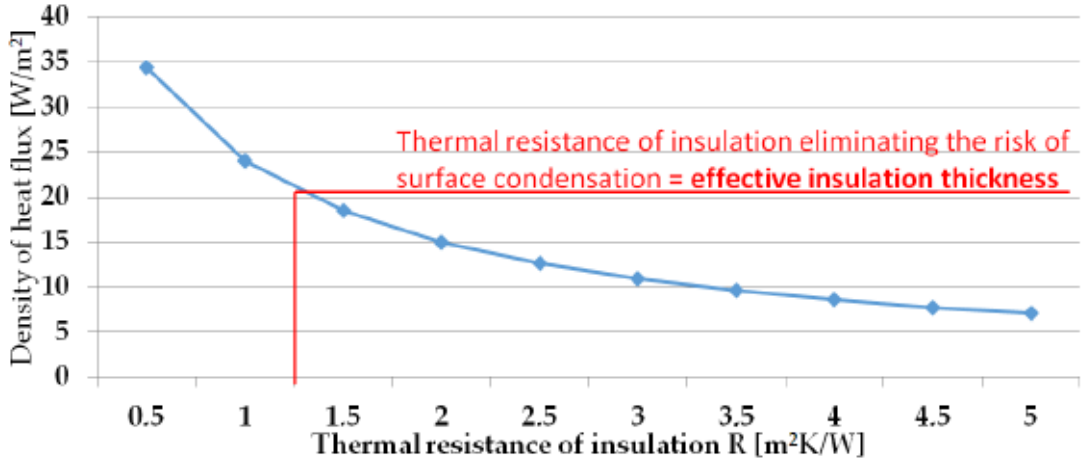

Figure 28.
Changes in heat flux density for a brick wall (38 cm) insulated with the material with thermal resistance of 0.5÷5.0 [m² K/W]

expressed by the effective factor f_{Rsi} and drying of the component layers of the analyzed wall system are met, Fig. 28. Although increasing the thickness of the insulation material allows to meet the minimum requirements as to the value of thermal transmittance coefficient U, but it limits the drying process of the envelope and reduces the intensity of heat flow coming from the adjacent zones, which also results in freezing of the elements in the node.

- all thermal insulation works should be carried out in accordance with the principle of primum non nocere (First, do no harm), which is often associated with the need to depart from the requirements set for thermal modernization works in mandatory regulations. For this reason, it is recommended to define separate requirements and criteria that would be imposed on historic buildings (currently, designing is carried out based on the same principles as for new buildings).
- the designed thermal insulation system from the inside should be assessed in terms of properly solved connections, for which the risk of mold development and moisture growth in individual layers of the node has been eliminated. The above conclusions apply to all nodes, although they were derived on the basis of the so-called geometric bridges.
- it seems reasonable to perform comprehensive calculations of connections in buildings insulated from the inside, which would be the basis for developing a catalog of such solutions, with particular emphasis on 3D connections.
- in effect of the presented work, we propose a procedure for designing connections and nodes in wall systems insulated from the inside, Fig. 29.

Figure 29. Procedure for selecting the type and thickness of insulation at the connections in wall systems insulated from the inside.

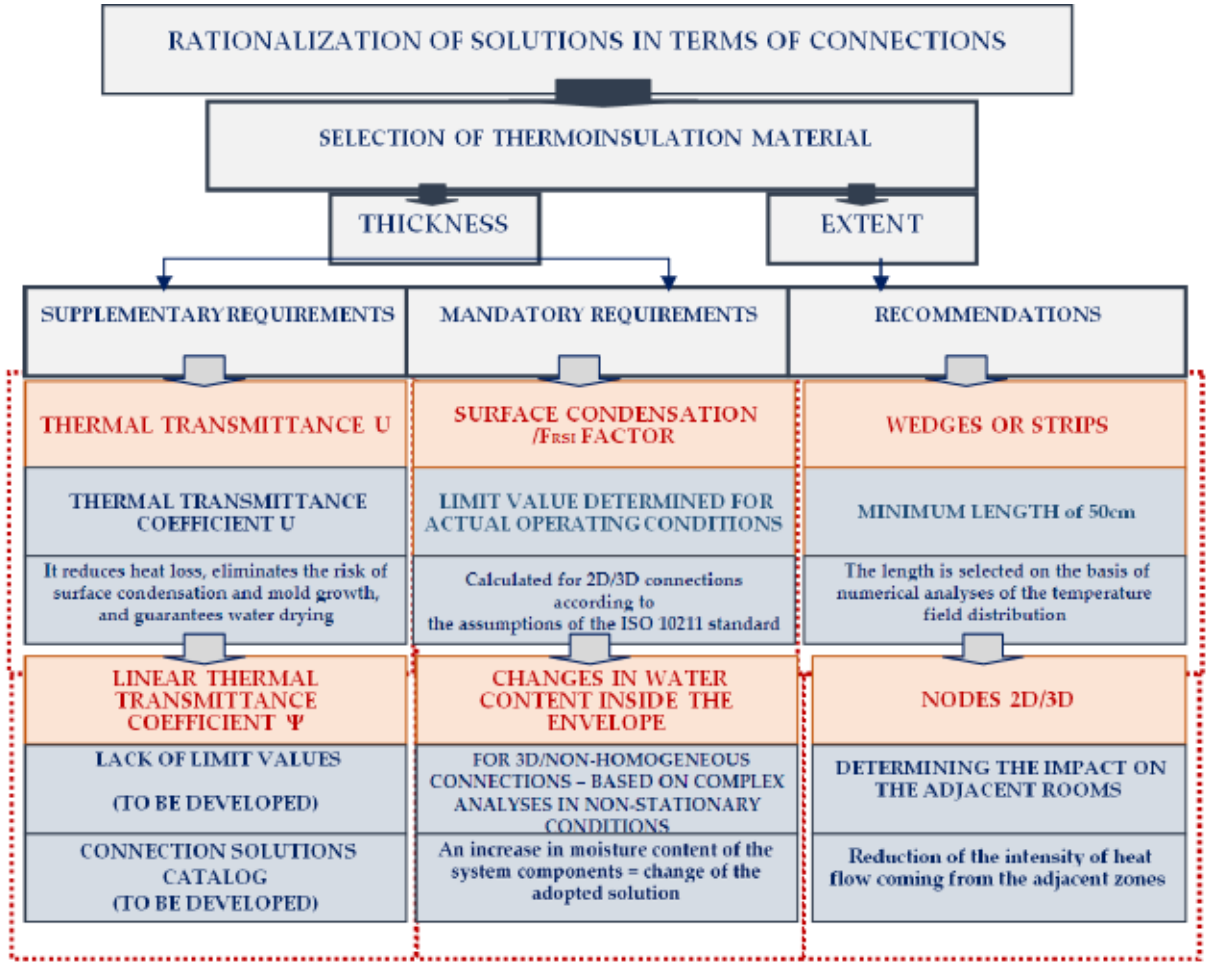

Figure 29.
Procedure for selecting the type and thickness of insulation at the connections in wall systems insulated from the inside

REFERENCES

[1] Ali K.A., Ahmad M.I., Yusup Y. (2020). Issues, impacts, and mitigations of carbon dioxide emissions in the building sector, *Sustainability* (Switzerland), *12*(18).

[2] Atmaca N., Atmaca A., Ali İhsan Özçetin (2021). The impacts of restoration and reconstruction of a heritage building on life cycle energy consumption and related carbon dioxide emissions, *Energy and Buildings*, 253.

[3] Sizirici B., Fseha Y., Cho C.S., Yildiz I., Byon Y.J. (2021). A review of carbon footprint reduction in construction industry, from design to operation, *Materials, 14*(20).

[4] Global Status Report, Towards a zero emission, efficient and resilient buildings and construction sector https://www.worldgbc.org/sites/default/files/2018%20GlobalABC%20Global%20Status%20Report.pdf

[5] https://ec.europa.eu/info/news/focus-energy-efficiency-buildings-2020-lut-17_en (access 21.10.21).

[6] Directive (EU) 2024/1275 of the European Parliament and of the Council of 24 April 2024 on the energy performance of buildings

[7] COMMISSION RECOMMENDATION (EU) 2021/1749 of 28 September 2021 on the Energy Efficiency First Principle: From Principles to Practice Guidance and Examples on its Implementation in Decision Making in the Energy Sector and in other sectors, https://eur-lex.europa.eu/legal- content/PL/TXT/PDF/?uri=CELEX:32021H1749&from=PL

[8] ITB instruction 447/2009: Complex thermal insulation systems for external walls of buildings ETICS, Principles of design and construction, Warsaw 2009.

[9] Arbeiter K. (2014). Innendammung; Auswahl, Konstruktion, Ausfuhhrung.

[10] Johansson P., Geving S., Hagentoft C.E., Jelle B.P., Rognvik E., Kalagasidis A.S., Time B. (2014): Interior insulation retrofit of a historical brick wall using vacuum insulation panels: Hygrothermal numerical simulations and laboratory investigations, *Building and Environment*, 79, 31–45

[11] Muller R. (2016). Fachverband Innendammung; Praxihandbuch Innendammung: Planung-Konstruktion – Details Beispiele.

[12] Orlik-Kożdoń B., Radziszewska-Zielina E., Fedorczak-Cisak M., Steidl T., Białkiewicz A., Żychowska M., Muzychak A. (2020). Historic building thermal diagnostics algorithm presented for the example of a townhouse in Lviv, *Energies, 13*(20).

[13] Orlik-Kożdoń B., Szymanowska-Gwiżdż A. (2018). Impact of envelope structure on the solutions of thermal insulation from the inside, *Architecture, Civil Engineering, Environment, 11*(4), 123–134.

[14] Orlik-Kożdoń B., Steidl T. (2017). Impact of internal insulation on the hygrothermal performance of brick wall, *Journal of Building Physics, 41*(2), 120–134.

[15] Zhou X., Derome D., Carmeliet J. (March 2022). Analysis of moisture risk in internally insulated masonry walls, *Building and Environment*, 15.

[16] Vereecken E., Roels S. (2014). A comparison of the hygric performance of interior insulation systems: A hot box-cold box experiment, *Energy and Buildings*, 80, 37–44.

[17] Walker R., Pavía S. (2018). Thermal and moisture monitoring of an internally insulated historic brick wall, *Building and Environment*, 133, 178–186.

[18] Worch A. (2009). Innendammung – Moglichkeiten und Grenzen, WTA-Schriftenreihe, 31.

[19] Worch A. (2012). Innendammung von einschaligem Ziegelmauerwerk, *Bausubstanz*, 3, 56–61.

[20] Zhao J., Grunewald J., Ruisinger U., Feng S. (2017). Evaluation of capillary active mineral insulation systems for interior retrofit solution, *Building and Environment*, 115, 215–227.

[21] Hansen W., Kung J.H. (1988). Pore structure and frost durability of clay bricks, *Materials and Structures/Matdriaux et Constructions,* 21, 443–447.

[22] Künzel H.M. (1998). Effect of interior and exterior insulation on the hygrothermal behaviour of exposed walls, *Materials and Structures*, 31, 99–103.

[23] Straube J., Schumacher C. (2007). Interior insulation retrofits of load-bearing masonry walls in cold climates, *In Journal of Green Building, 2*(2), 42–50.

[24] Vereecken E., Van Gelder L., Janssen H., Roels S. (2015). Interior insulation for wall retrofitting. A probabilistic analysis of energy savings and hygrothermal risks, *Energy and Buildings*, 89, 231 244.

[25] Wójcik R., Bomberg M. On interior rehabilitation of buildings with historic facades, *Journal of Building Physics, 40*(2), 144–161.

[26] Guizzardi M., Carmeliet J., Derome D. (2015). Risk analysis of biodeterioration of wooden beams embedded in internally insulated masonry walls, *Construction and Building Materials*, 99, 159–168.

[27] Morelli M., Svendsen S. (2013). Investigation of interior post-insulated masonry walls with wooden beam ends, *Journal of Building Physics, 36*(3), 265–273.

[28] Viitanen H., Salonvaara M. (). Moisture conditions and biodeterioration risk of building materials and structure, https://www.researchgate.net/publication/228735301_Moisture_conditions_and_biodeterioration_risk_of_building_materials_and_structure (access 9.02.2020).

[29] Krause P., Nowoświat A., Pawłowski K. (2020). The impact of internal insulation on heat transport through the wall: case study, *Applied Sciences-Basel, MDPI, 10*(21).

Standards and related documents:

[30] Orlik-Kożdoń B. (2022). Forecasting moisture condition of walls insulated from the inside in historic brick buildings, Gliwice.

[31] Scheffler A.G. (2015). Bauphysik der Innendammung, Frauhofer IRB.

[32] Wyrwał J., Marynowicz A. (2002). Vapour condensation and moisture accumulation in porous building wall, *Building and Environment, 37*(3), 313–318.

[33] Regulation of the Minister of Infrastructure on the technical conditions to be met by buildings and their location. Regulation of April 12, 2002. (Journal of Laws of 2019, item 1065), Unified text – taking into account the introduced amendments (Journal of Laws of September 16, 2020, item 1608).

[34] Orlik-Kożdoń B. (2019). Interior insulation of masonry walls-selected problems in the design, *Energies, 12*(20), 1–22.

[35] Orlik-Kożdoń B. (2020). Microclimate conditions in rooms: Their impact on mold development in buildings, *Energies, 13*(17).

[36] ISO 10211: 2017 9: Thermal bridges in building construction – Heat flows and surface temperatures – Detailed calculations.

[37] ISO 13788: 2013 Hygrothermal performance of building components and building elements – Internal surface temperature to avoid critical surface humidity and interstitial condensation – Calculation methods.